Preclinical Development of a Bifunctional Cancer Cell Homing, PKCε Inhibitory Peptide for the Treatment of Head and Neck Cancer

Liwei Bao,[1] Michael A. Gorin,[3] Manchao Zhang,[4] Alejandra C. Ventura,[1] William C. Pomerantz,[2] Sofia D. Merajver,[1] Theodoros N. Teknos,[4,5] Anna K. Mapp,[2] and Quintin Pan[4,5]

[1]Department of Internal Medicine, Division of Hematology and Oncology, University of Michigan Medical School; [2]Department of Chemistry, University of Michigan, Ann Arbor, Michigan; [3]Miller School of Medicine, University of Miami, Miami, Florida; and [4]Arthur G. James Cancer Hospital and Richard J. Solove Research Institute, The Ohio State University Comprehensive Cancer Center; [5]Department of Otolaryngology-Head and Neck Surgery, The Ohio State University Medical Center, Columbus, Ohio

Abstract

Head and neck squamous cell carcinoma (HNSCC) is the sixth most frequent cancer worldwide, comprising ~50% of all malignancies in some developing nations. Our recent work identified protein kinase Cε (PKCε) as a critical and causative player in establishing an aggressive phenotype in HNSCC. In this study, we investigated the specificity and efficacy of HN1-PKCε, a novel bifunctional cancer cell homing, PKCε inhibitory peptide, as a treatment for HNSCC. HN1-PKCε peptide was designed by merging two separate technologies and synthesized as a capped peptide with two functional modules, HN1 (cancer cell homing) and PKCε (specific PKCε inhibitory), connected by a novel linker module. HN1-PKCε preferentially internalized into UMSCC1 and UMSCC36 cells, two HNSCC cell lines, in comparison with oral epithelial cells: 82.1% positive for UMSCC1 and 86.5% positive for UMSCC36 compared with 1.2% positive for oral epithelial cells. In addition, HN1-PKCε penetrated HNSCC cells in a dose- and time-dependent manner. Consistent with these *in vitro* observations, systemic injection of HN1-PKCε resulted in selective delivery of HN1-PKCε into UMSCC1 xenografts in nude mice. HN1-PKCε blocked the translocation of active PKCε in UMSCC1 cells, confirming HN1-PKCε as a PKCε inhibitor. HN1-PKCε inhibited cell invasion by 72 ± 2% ($P < 0.001$, $n = 12$) and cell motility by 56 ± 2% ($P < 0.001$, $n = 5$) in UMSCC1 cells. Moreover, *in vivo* bioluminescence imaging showed that HN1-PKCε significantly (83 ± 1% inhibition; $P < 0.02$) retards the growth of UMSCC1 xenografts in nude mice. Our work indicates that the bifunctional HN1-PKCε inhibitory peptide represents a promising novel therapeutic strategy for HNSCC. [Cancer Res 2009;69(14):5829–34]

Introduction

Head and neck squamous cell carcinoma (HNSCC) is the sixth most frequent cancer worldwide. Nearly 46,000 people will be diagnosed with HNSCC in the United States this year and an estimated 11,000 people will die of the disease (1). Although improvements in local control and survival have been achieved with the use of multimodality regimens, the overall 5-year survival rate for HNSCC has not improved significantly over the past 20 years (2, 3). Local-regional relapse and distant metastasis after definitive therapy remain the major causes of morbidity and mortality in HNSCC patients. This clinical problem has prompted substantial efforts in identifying genetic determinants that contribute to aggressive HNSCC.

Evidence has shown that protein kinase Cε (PKCε), a member of a family of serine/threonine protein kinases, is a transforming oncogene and is involved in the development and progression of skin, breast, and prostate cancer (4–6). Our recent results show that PKCε plays a critical and causative role in establishing an aggressive phenotype in HNSCC. We reported that PKCε is upstream of and directly modulates the Rho GTPase signaling cascade, specifically RhoA and RhoC, to control cell invasion and motility (7). Moreover, specific inhibition of PKCε with RNA interference in HNSCC cells with high endogenous PKCε levels was sufficient to significantly inhibit cell invasion and motility (7). A prospective study showed that elevated PKCε in the primary tumor of HNSCC patients is associated with an increase in disease recurrence and a decrease in overall survival (8). This observation agrees with our work that PKCε promotes an aggressive phenotype in HNSCC and suggests that targeting PKCε may be an effective anticancer strategy for managing HNSCC patients.

In this study, we determined the effects of a novel cancer cell homing, PKCε inhibitory peptide on HNSCC cells *in vitro* and *in vivo*. The bifunctional HN1-PKCε peptide was constructed by connecting two functional motifs, HN1 (cancer cell homing) and PKCε (specific PKCε inhibitory), with a linker peptide. HN1-PKCε preferentially penetrated HNSCC cells *in vitro* and *in vivo* and blocked the translocation of active PKCε in HNSCC cells. In addition, HN1-PKCε inhibited cell invasion, motility, and proliferation *in vitro* and significantly retarded the growth of HNSCC xenografts in nude mice. Our work shows that HN1-PKCε is a novel therapeutic agent with potent antitumor efficacy against HNSCC.

Materials and Methods

Cell lines. Immortalized normal oral epithelial cells (E6/E7-NOE) were kindly provided by Drs. William Foulkes and Ala-Eddin Al Moustafa (McGill University) and cultured in keratinocyte serum-free medium without supplement. UMSCC1 and UMSCC36 cells were kindly provided by Dr. Thomas Carey (University of Michigan Medical School) and cultured in DMEM supplemented with 10% fetal bovine serum.

Peptide synthesis. Unlabeled and FITC-labeled peptides were synthesized and purified (>95%) by the University of Michigan Protein Structure and Peptide Synthesis Facility or by New England Peptides. Cy5-labeled HN1-PKCε was synthesized and purified (>95%) by Open Biosystems. Cy5-labeled PKCε was synthesized by standard *N*-9-fluorenylmethoxycarbonyl (Fmoc) solid-phase synthesis on CLEAR amide resin (0.48 mmol/g; Peptide International). Following Fmoc deprotection of the final residue, 2 equivalents of Cy5-NHS ester (GE Healthcare) and 4 equivalents of triethylamine were dissolved in NMP and transferred to the resin. The

Requests for reprints: Quintin Pan, Department of Otolaryngology-Head and Neck Surgery, The Ohio State University Medical Center, Cramblett Medical Clinic-Suite 4A, 456 West Tenth Avenue, Columbus, OH 43210. Phone: 614-247-4438; Fax: 614-688-4761; E-mail: Quintin.Pan@osumc.edu.

doi:10.1158/0008-5472.CAN-08-3465

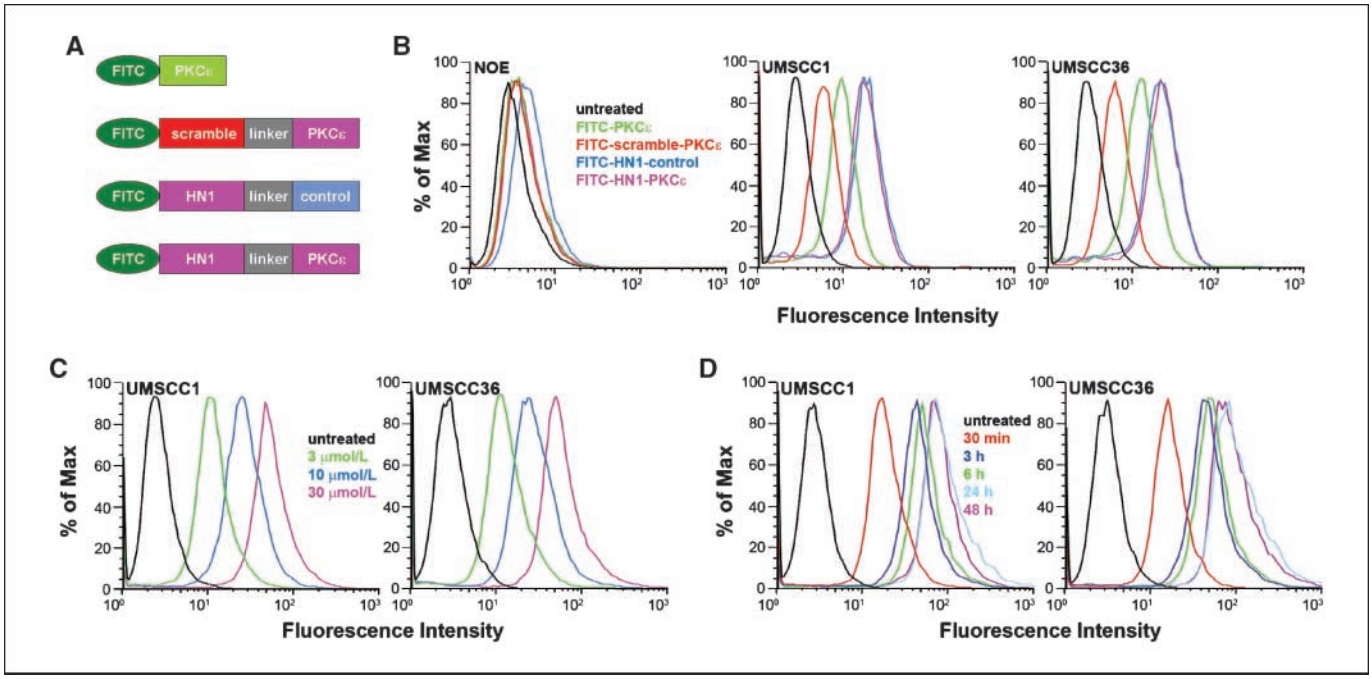

Figure 1. HN1-PKCε selectively penetrates HNSCC cells *in vitro*. *A,* schematic diagram of FITC-labeled peptides. HN1 module: cancer cell homing peptide. Scrambled module: nonfunctional scrambled HN1 module. Linker module: linker peptide. PKCε module: PKCε inhibitory peptide. Control module: nonfunctional scrambled PKCε module. Peptides were end capped (5′-acetylated and 3′-amidated) to enhance stability. *B,* HN1-PKCε preferentially internalizes into HNSCC *in vitro*. NOE cells and HNSCC cells, UMSCC1 and UMSCC36, were untreated or incubated with FITC-labeled peptides (3 μmol/L) for 48 h. Cells were harvested and analyzed by FACS. *C,* dose-dependent internalization of HN1-PKCε into HNSCC cells. UMSCC1 and UMSCC36 cells were untreated or incubated with 3, 10, or 30 μmol/L of HN1-PKCε for 48 h. Cells were harvested and analyzed by FACS. *D,* time-dependent internalization of HN1-PKCε into HNSCC cells. UMSCC1 and UMSCC36 cells were untreated or incubated with 30 μmol/L HN1-PKCε for 30 min and 3, 6, 24, or 48 h. Cells were harvested and analyzed by FACS. These histograms are representative of several independent experiments.

reaction vessel was covered in foil and left to react for 16 h. The resin was washed thrice with DMF, thrice with CH_2Cl_2, and thrice with methanol. The Cy5-labeled PKCε peptide was cleaved from the resin for 2 h in a mixture of 95/2.5/2.5 trifluoroacetic acid (TFA)/triisopropylsilane/water. The crude peptide was precipitated into cold ether and purified by reversed-phase high-performance liquid chromatography on a Waters C18 column using water with 0.1% TFA as the A solvent and CH_3CN as the B solvent (14%-31% B over 17 min). Product molecular weight was confirmed by electrospray-mass spectrometry in both negative ion mode (m-H^+, 1,479.1) and positive ion mode (M+2H^+/2, 740.9).

PKCε translocation. UMSCC1 cells were untreated or treated with HN1-control or HN1-PKCε for 48 h. Subsequently, cells were stimulated with a general PKC activator, phorbol 12-myristate 13-acetate (PMA; 10 nmol/L for 30 min), washed with cold PBS, scraped in homogenization buffer (9), passed through a 25-gauge syringe needle, and spun at 100,000 × *g* for 30 min at 4°C. The cytoplasmic fractions were collected and the pellets (particulate fractions) were resuspended in homogenization buffer with 1% Triton X-100. Western blot analysis using a PKCε-specific antibody (Millipore) was performed to assess the translocation of PKCε.

Cell invasion and cell motility. Cell invasion was determined as described from the cell invasion assay kit (Chemicon International). Cells were harvested and resuspended in serum-free medium. An aliquot (1×10^5 cells) of the prepared cell suspension was added into the chamber and incubated for 24 h at 37°C in a 10% CO_2 tissue culture incubator. Noninvading cells were gently removed from the interior of the inserts with a cotton-tipped swab. Invasive cells were stained and counted. Random cell motility was determined as described from the motility assay kit (Cellomics). Cells were harvested, suspended in medium, and plated on top of a field of microscopic fluorescent beads. After a 16-h incubation period, cells were fixed and areas of clearing in the fluorescent bead field corresponding to phagokinetic cell tracks were quantified using NIH ScionImager.

Cell proliferation. Cells were untreated or treated with *cis*-platinum (1, 3, or 10 μmol/L), *cis*-platinum and HN1-control, or *cis*-platinum and HN1-PKCε for 3 d. Cell proliferation was assessed using the 3-(4,5-dimethylthiazol-2-yl)-2,5-diphenyltetrazolium bromide (MTT) reagent to detect metabolic active cells (Sigma).

Preclinical efficacy of HN1-PKCε. UMSCC1-luciferase cells (1×10^6) were implanted into the flank of 10-wk-old athymic nude mice and tumors were allowed to develop without treatment. At 2 wk after implantation, mice with established tumors of ~40 mm^3 in volume were imaged for bioluminescence intensity using the Xenogen IVIS Spectrum System (Caliper Life Sciences). Mice were randomly assigned to three treatment arms, untreated (n = 9), HN1-control (10 mg/kg, thrice weekly, n = 8), or HN1-PKCε (10 mg/kg, thrice weekly, n = 11), based on bioluminescence intensity to achieve a statistically similar mean bioluminescence intensity at the start of the treatment protocol. Tumor response was assessed on a weekly basis using the *in vivo* bioluminescence imaging modality.

Statistical analysis. Data were analyzed by Student's t test. P values of <0.05 were considered significant.

Results and Discussion

The excitement over PKCs as therapeutic anticancer targets prompted the rapid development of drugs designed to specifically inhibit PKCs. The drugs developed to date can be divided into two main groups: inhibitors that target the C1 regulatory domain and inhibitors that target the kinase domain. Overall, in numerous clinical trials, PKC inhibitors have shown very modest activity, at best, as single agent or in combination with standard chemotherapeutics (10, 11). Bryostatin-1, a PKC modulator that targets the C1 domain, is the most extensively used in clinical trials. Recent phase II clinical trials with bryostatin-1 in combination with cisplatin for cervical squamous cell carcinoma or in combination

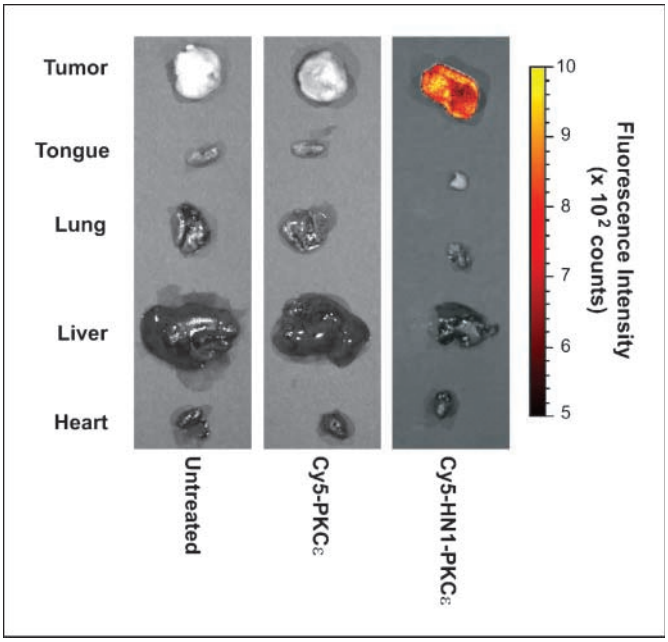

Figure 2. HN1-PKCε selectively homes to HNSCC xenografts *in vivo*. Nude mice with established UMSCC1 tumors in the flank were untreated or treated with Cy5-labeled HN1-control or HN1-PKCε (i.p. injection, 10 mg/kg). After 24 h, mice were euthanized and tumors and various organs were resected for fluorescence intensity analysis using the Xenogen IVIS Spectrum Imaging System.

with interleukin-2 for renal cell carcinoma showed minimal efficacy and perhaps even a possibility of therapeutic antagonism (12, 13). One possible explanation is that C1 domain inhibitors are not isoform specific because the C1 domain is well conserved in the PKC family, with the exception of the atypical isoforms. Therefore, C1 domain inhibitors likely inhibit desired oncogene-like PKC isoforms but also have the undesired side effect of inhibiting tumor suppressor–like PKC isoforms, resulting in no net response or possibly a tumor stimulatory response. The kinase domain inhibitors are not specific PKC inhibitors because the kinase inhibitors target other serine/threonine kinases with higher specificity. Taken together, there remains a critical need to develop isoform-specific PKC inhibitors.

The activation of the PKCε signaling cascade is a critical genetic event resulting in an aggressive HNSCC phenotype. Our laboratory reported that RhoA and RhoC are directly phosphorylated by PKCε, resulting in an increase in RhoA/RhoC activation (7). In addition to regulation of RhoA and RhoC, other groups have published that PKCε directly phosphorylates Akt and Stat3. PKCε phosphorylates Akt at Ser^{473} leading to a full Akt activation state (14). A recent report showed that PKCε phosphorylates Stat3 at Ser^{727}, resulting in an increase in nuclear translocation and transcriptional activation of Stat3 (15). Elevated Akt phosphorylation (Ser^{473}) significantly correlates with a worse outcome in HNSCC (16, 17). Nuclear Stat3 accumulation is associated with a decrease in relapse-free and overall survival in HNSCC (18). Thus, targeting PKCε is an attractive therapeutic strategy, as inhibition of PKCε will result in dampening of multiple signal transduction pathways that are dysregulated in HNSCC.

Protein-protein interactions are critical events in numerous signaling pathways. However, because protein to protein interfaces are usually extensive, shallow, and hydrophobic, the disruption of protein-protein interactions has proven to be difficult targets for small-molecule drugs. So, we decided to take a different approach and rationally designed a bifunctional targeting peptide. We merged two existing and published technologies and constructed a peptide with two functional modules, HN1 and PKCε, connected by a linker module. The HN1 module is a 12-mer peptide,

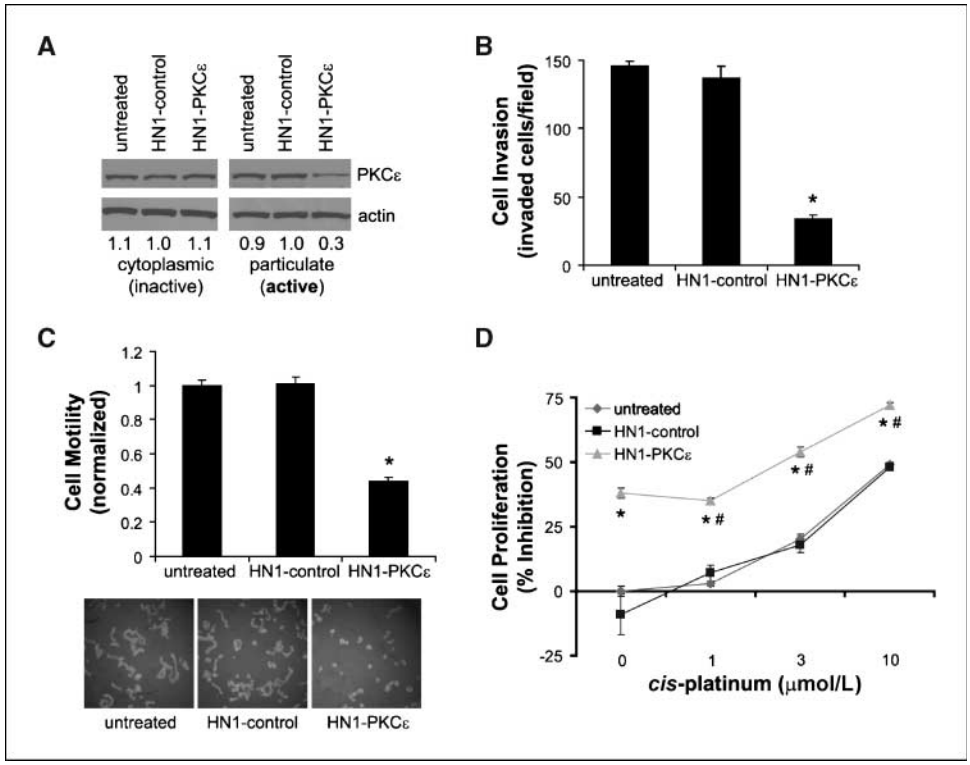

Figure 3. HN1-PKCε blocks active PKCε translocation and inhibits cell invasion, motility, and proliferation. *A,* HN1-PKCε disrupts localization of active PKCε in HNSCC cells. Inactive and active PKCε levels were detected by Western blot analysis with an anti-PKCε antibody. Bands were quantified by densitometry and data are presented as fraction of PKCε levels relative to the HN1-control–treated cells. *B,* HN1-PKCε inhibits cell invasion. Cell invasion was assessed using the modified Boyden chamber invasion assay with Matrigel basement membrane. Invasive cells were counted and presented as invaded cells per field. *, $P < 0.001$ ($n = 12$). *C,* HN1-PKCε inhibits cell motility. Cell motility was assessed using the two-dimensional random cell motility assay. Cells were fixed and areas of clearing in the microbead field corresponding to phagokinetic cell tracks were quantified using NIH ScionImager. *, $P < 0.001$ ($n = 5$). *D,* HN1-PKCε inhibits cell proliferation. Cell proliferation was determined using the MTT assay. *, $P < 0.006$ ($n = 4$), HN1-PKCε compared with HN1-control or *cis*-platinum; #, $P < 0.001$ ($n = 4$), monotherapy HN1-PKCε compared with combination regimen of HN1-PKCε and *cis*-platinum.

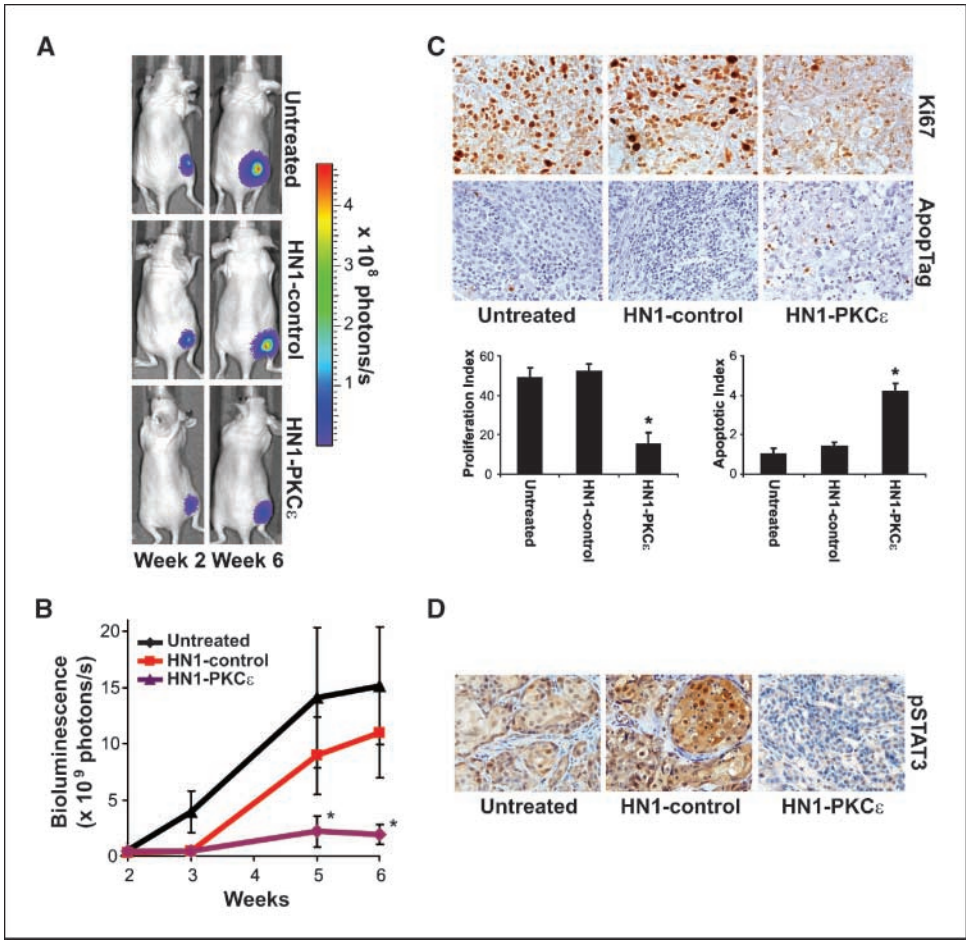

Figure 4. HN1-PKCε retards tumor growth in a preclinical model of HNSCC. *A,* bioluminescence images from a representative mouse in the untreated arm, HN1-control treatment arm, and HN1-PKCε treatment arm. *B,* bioluminescence. Tumor bioluminescence activity was measured using the Xenogen IVIS Spectrum Imaging System. *, $P < 0.02$. *C,* tumor proliferation and apoptotic index. Tumor sections were stained for proliferating cells using an anti-Ki67 antibody (DAKO) and apoptotic cells using the ApopTag kit (InterGen Co.). Proliferation and apoptotic index was determined by counting the number of Ki67-positive and terminal deoxynucleotidyl transferase–mediated dUTP nick end labeling–positive cells per 500 total cells in five separate random fields at high power. Magnification, ×400. *, $P < 0.001$. *D,* tumor pStat (S727) levels. Tumor sections were stained for S727-phosphorylated Stat3 using an anti-phospho-S727-Stat3 antibody (Cell Signaling). These are representative sections for each treatment arm.

TSPLNIHNGQKL, reported to preferentially bind and internalize into HNSCC cell lines *in vitro* (19). Moreover, HN1 was shown to be stable *in vivo* and able to localize into HNSCC xenograft tumors (19). The PKCε inhibitory module (εV1-2) is an 8-mer peptide, EAVSLKPT, taken from amino acids 14 to 21 located in the pseudo-C2 domain of PKCε (20). There is literature to show that the pseudo-C2 domain of PKCε is required for binding to receptors of activated PKC (RACK; refs. 21, 22). The PKCε-RACK interaction allows for the proper trafficking and localization of active PKCε (21, 22). The RACK binding site on PKCε was reported to be a discrete region located at amino acids 14 to 21 (20). A peptide (εV1-2) corresponding to this sequence inhibited the translocation and function of active PKCε through blocking the PKCε-RACK interaction in cardiac myocytes (20). Moreover, εV1-2 was shown to be a specific PKCε inhibitor and not able to block the translocation and function of other PKCs, specifically PKCα, PKCβ and PKCδ (20). Subsequent work has clearly shown that εV1-2 is a specific PKCε inhibitor in other cell types, including neuronal cells and pancreatic β-cells (23, 24). The control module is a nonfunctional scrambled PKCε peptide, LSETKPAV (20). The linker module consists of a 6-mer sequence of 6-aminohexanoic acid to allow for proper spatial spacing to prevent steric interference between the HN1- and PKCε-targeting modules.

To determine the efficiency and selectivity of HN1-PKCε for HNSCC cells *in vitro*, oral epithelial cells (NOE), UMSCC1, and UMSCC36 were untreated or treated with a series of different FITC-labeled peptides (3 μmol/L for 48 hours) followed by fluorescence-activated cell sorting (FACS) analysis (Fig. 1*A*). NOE cells treated with FITC-labeled HN1-PKCε had minimal effect and resulted in 1.2% FITC-positive cells with a mean fluorescence intensity of 1.9. In contrast, FITC-labeled HN1-PKCε treatment of UMSCC1 and UMSCC36 cells resulted in 82.1% and 86.5% FITC-positive cells, respectively. The mean fluorescence intensity was 15.9 for UMSCC1 cells and 18.3 for UMSCC36 cells with FITC-labeled HN1-PKCε treatment. As expected, treatment with FITC-labeled scramble-PKCε, a peptide with an inactive cancer cell homing module, was not as efficient and resulted in 10.2% FITC-positive cells for UMSCC1 and 5.3% FITC-positive cells for UMSCC36. It is clear that FITC-labeled HN1-PKCε is >8-fold more efficient ($P < 0.03$) than FITC-labeled scramble-PKCε, providing evidence that the addition of the functional HN1 cancer cell homing module is a critical value-added feature to enhance the uptake of the PKCε inhibitory module in HNSCC cells. Treatment with FITC-labeled HN1-control had a similar effect as FITC-labeled HN1-PKCε and resulted in 82.6% FITC-positive cells for UMSCC1 and 82.7% FITC-positive cells for UMSCC36. This is an important observation and shows that modification of the amino acid sequence order of the PKCε inhibitory module to a nonfunctional scrambled control version does not alter the internalization efficiency into HNSCC cells. Interestingly, FITC-labeled PKCε is more efficient than FITC-labeled scramble-PKCε. A likely explanation is that the uptake of FITC-labeled peptides into HNSCC cells is mass/size dependent because FITC-labeled scramble-PKCε consists of 26 amino acid residues and FITC-labeled PKCε consists of

only 8 amino acid residues. Nonetheless, the internalization efficiency of FITC-labeled HN1-PKCε is superior to FITC-labeled PKCε ($P < 0.04$). Lastly, as shown in Fig. 1*C* and *D*, a dose- and time-dependent uptake of FITC-labeled HN1-PKCε was observed in UMSCC1 and UMSCC36 cells.

Next, we examined if HN1-PKCε specifically localizes to HNSCC tumors *in vivo*. We decided to use Cy5 as the fluorophore for this experiment because Cy5 exhibits longer excitation and emission wavelengths than FITC and, thus, enables deeper tissue penetration. Athymic nude mice with established UMSCC1 tumors in the flank were untreated or treated with Cy5-labeled PKCε or HN1-PKCε (10 mg/kg by i.p. injection). After 24 hours, mice were euthanized and tumors and various organs were resected for fluorescence intensity analysis using the Xenogen IVIS Spectrum Imaging System (Fig. 2). *Ex vivo* analysis showed that the tumors and various organs resected from untreated or Cy5-labeled PKCε-treated mice exhibit minimal fluorescence. In contrast, Cy5-labeled HN1-PKCε was selectively delivered to the HNSCC tumor. Fluorescence intensity was >8-fold higher ($P < 0.0001$) in the tumor compared with the various organs in Cy5-labeled HN1-PKCε–treated mice. These results showed that HN1-PKCε selectively homed to and penetrated into HNSCC tumors *in vivo*.

Our work corroborated the findings from Hong and Clayman (19) and showed that the HN1 motif selectively homes and penetrates HNSCC cells in comparison with immortalized oral epithelial cells. Furthermore, we have evidence that HN1-PKCε does not internalize into primary keratinocytes (data not shown). Hong and Clayman (19) reported that HN1 did not internalize into DU145 human prostate cancer cells, SW480 human colon cells, and U373 MG human astrocytoma cells, suggesting that HN1 may be specific to squamous cell carcinoma. However, this is not the case as HN1-PKCε efficiently internalized into MDA-MB231 (70.1% FITC positive; mean fluorescence intensity of 64.2) and SKBR3 (49.4% FITC positive; mean fluorescence intensity of 27.3) human breast cancer cells. Interestingly, HN1-PKCε penetrated MCF10A non-tumorigenic mammary epithelial cells with much lower efficiency (8.8% FITC positive; mean fluorescence intensity of 5.9). These results provide initial evidence that HN1 may be cancer cell specific but not organ specific. Our observations do not detract from the significance and utility of HN1 but rather expands the potential clinical use of HN1 to other cancer types.

The PKCε inhibitory module was shown to selectively block the translocation of active PKCε in numerous cell types, including cardiac myocytes, pancreatic β-cells, and neuronal cells (19, 23, 24). There is evidence to indicate that inactive PKCε is localized in the cytoplasmic fraction and on activation translocates to the particulate fraction (25, 26). To determine if HN1-PKCε can block the translocation of active PKCε in HNSCC cells, UMSCC1 cells were untreated or incubated with HN1-control or HN1-PKCε for 24 hours. Subsequently, cells were activated with PMA and cell lysates were fractionated for cytoplasmic and particulate proteins. As shown in Fig. 3*A*, active PKCε is dramatically lower in HN1-PKCε–treated cells than in untreated or HN1-control–treated cells. These results provide direct evidence that HN1-PKCε disrupts the proper localization of PKCε, resulting in "normalization" of active PKCε levels in HNSCC cells.

We determined the effects of HN1-PKCε on cell invasion, cell motility, and cell proliferation. UMSCC1 cells were untreated or incubated with 30 μmol/L HN1-control and HN1-PKCε for 72 hours. Subsequently, cells were trypsinized and replated in appropriate experimental wells to assess for cell invasion and cell motility. UMSCC1 cells treated with HN1-PKCε were significantly less invasive and motile than untreated cells or HN1-control–treated cells (Fig. 3*B* and *C*). HN1-PKCε inhibited cell invasion by 72 ± 2% ($P < 0.001$, $n = 12$) and cell motility was suppressed by 56 ± 2% ($P < 0.001$, $n = 5$) in UMSCC1 cells. As shown in Fig. 3*D*, the effects of HN1-PKCε on cell proliferation as monotherapy or in combination therapy with *cis*-platinum were assessed. As expected, *cis*-platinum (no peptide treatment) inhibited cell proliferation in a dose-dependent manner, ranging from 3 ± 1% inhibition for 1 μmol/L to 49 ± 2% inhibition for 10 μmol/L. HN1-control (30 μmol/L for 72 hours) had no effect on cell proliferation as monotherapy, and no additional effect was observed in combination with *cis*-platinum. Single-agent treatment of HN1-PKCε (30 μmol/L for 72 hours) significantly inhibited cell proliferation by 39 ± 2%, and, moreover, used in a combination treatment regimen, an additive effect is observed with *cis*-platinum. Single-agent *cis*-platinum (10 μmol/L for 72 hours) inhibited cell proliferation by 49 ± 2%, whereas the combination regimen of 30 μmol/L HN1-PKCε and 10 μmol/L *cis*-platinum for 72 hours inhibited cell proliferation by 72 ± 4%. The combination regimen resulted in a 47% increase in inhibition of cell proliferation compared with single-agent *cis*-platinum treatment. This observation supports the notion that the combination regimen of a PKCε inhibitor and *cis*-platinum is more efficacious than either single-agent therapy alone. It is critical to point out that the HN1 module does not have anticancer properties, as the HN1-control peptide had no effect on cell invasion, motility, and proliferation. These observations strongly indicate that the PKCε inhibitory module is solely responsible for the antitumor effects as observed in these phenotypic experiments.

The antitumor efficacy of HN1-PKCε was assessed in a xenograft model of HNSCC. UMSCC1 cells were infected with a lentivirus expression vector to drive constitutive *Firefly* luciferase (pLentilox-Luc) to allow us to measure tumor response using a highly sensitive and dynamic *in vivo* bioluminescence imaging modality. UMSCC1-luciferase cells (1×10^6) were implanted into the flank of 10-week-old athymic nude mice, and tumors were allowed to develop without treatment. At 2 weeks after implantation, mice with established tumors of ~40 mm^3 in volume were imaged for bioluminescence intensity. Mice were randomly assigned to three treatment groups, untreated ($n = 9$), HN1-control (10 mg/kg i.p. injection, thrice weekly, $n = 8$), or HN1-PKCε (10 mg/kg i.p. injection, thrice weekly, $n = 11$), based on bioluminescence intensity to achieve a statistically similar mean bioluminescence intensity at the start of the treatment protocol. At the end of the 4-week treatment protocol, mean tumor bioluminescence intensity between the untreated arm and HN1-control–treated arm was statistically similar ($P > 0.05$): 15.2 ± 5.2 photons/s for the untreated mice and 11.0 ± 3.9 photons/s for the HN1-control–treated mice (Fig. 4*B*). Mice from the HN1-PKCε treatment arm showed a dramatic difference and had a mean tumor bioluminescence intensity of only 1.9 ± 0.9 photons/s. Mean tumor bioluminescence intensity was ~5.8-fold higher in the HN1-control arm in comparison with the HN1-PKCε arm ($P < 0.02$). As shown in Fig. 4*C*, immunohistochemical staining indicated that HN1-PKCε treatment resulted in a 71 ± 8% decrease in the tumor proliferation index and a 314 ± 29% increase in the tumor apoptotic index compared with HN1-control treatment ($P < 0.001$). Additionally, pStat3 (S727) levels, a downstream target of active PKCε, were markedly lower in the tumors from the HN1-PKCε arm than from the untreated or HN1-control arm. These *in vivo*

results show a robust antitumor effect with HN1-PKCε treatment in HNSCC.

The paradigm of molecularly targeted anticancer therapies is beginning to take hold. To date, several molecularly targeted anticancer therapies, such as bevacizumab and cetuximab, have proven to be effective approaches for managing cancer patients. Many of these molecularly targeted anticancer agents have shown to be more selective for cancer cells and thus exhibit lower overall toxicity profiles than standard chemotherapeutics. Nevertheless, dose-limiting toxicities, most likely due to drug delivery to nontarget cells and organs, remain a critical issue even with molecularly targeted anticancer drugs. Development of a bifunctional anticancer drug consisting of a molecularly targeted therapeutic and a tumor-targeting component will enable the specific delivery of an anticancer therapeutic to tumor cells, resulting in increased local efficacy while limiting peripheral toxicity. HN1-PKCε was conceived with these two criteria in mind. Our results clearly show that HN1-PKCε is functioning as designed and selectively penetrates HNSCC cells to inhibit active PKCε translocation. Systemic administration of HN1-PKCε significantly retarded the growth of HNSCC xenograft as measured by a highly sensitive *in vivo* bioluminescence imaging modality. There was no apparent difference in the weight of untreated, HN1-control–treated, and HN1-PKCε–treated mice during the active treatment period, providing initial evidence that HN1-PKCε has a favorable toxicity profile. Taken together, this study indicates that HN1-PKCε has potent antitumor effects and further development of HN1-PKCε as an anticancer therapeutic for HNSCC is warranted.

Disclosure of Potential Conflicts of Interest

No potential conflicts of interest were disclosed.

Acknowledgments

Received 9/5/08; revised 5/12/09; accepted 5/14/09; published OnlineFirst 6/30/09.

Grant support: National Cancer Institute grants P50CA97248 (S.D. Merajver, T.N. Teknos, and Q. Pan), R01CA77612 (S.D. Merajver), and R01CA135096 (Q. Pan), Flight Attendant Medical Research Institute (Q. Pan), Burroughs Wellcome Trust (S.D. Merajver), and Department of Defense Breast Cancer Research Program (A.C. Ventura).

The costs of publication of this article were defrayed in part by the payment of page charges. This article must therefore be hereby marked *advertisement* in accordance with 18 U.S.C. Section 1734 solely to indicate this fact.

References

1. Jemal A, Siegel R, Ward E, Murray T, Xu J, Thun MJ. Cancer statistics, 2007. CA Cancer J Clin 2007;57:43–66.
2. Funk GF, Karnell LH, Robinson RA, Zhen WK, Trask DK, Hoffman HT. Presentation, treatment, and outcome of oral cavity cancer: a National Cancer Data Base report. Head Neck 2002;24:165–80.
3. Pugliano FA, Piccirillo JF, Zequeria MR, Fredrickson JM, Perez CA, Simpson JR. Clinical severity staging system for oral cavity cancer: five year survival. Otolaryngol Head Neck Surg 1999;120:38–45.
4. Jansen AP, Verwiebe EG, Dreckschmidt NE, Wheeler DL, Oberley TD, Verma AK. Protein kinase C-ε transgenic mice: a unique model for metastatic squamous cell carcinoma. Cancer Res 2001;61:808–12.
5. Pan Q, Bao LW, Kleer CG, et al. Protein kinase Cε is a predictive biomarker of aggressive breast cancer and a validated target for RNA interference anti-cancer therapy. Cancer Res 2005;65:8366–71.
6. Wu D, Foreman TL, Gregory CW, et al. Protein kinase Cε has the potential to advance the recurrence of human prostate cancer. Cancer Res 2002;62:2423–9.
7. Pan Q, Bao LW, Teknos TN, Merajver SD. Targeted disruption of PKCε reduces cell invasion and motility through inactivation of RhoA and RhoC GTPases in head and neck squamous cell carcinoma. Cancer Res 2006;66:9379–84.
8. Martinez-Gimeno C, Diaz-Meco MT, Dominguez I, Moscat J. Alterations in levels of different protein kinase C isotypes and their influence on behavior of squamous cell carcinoma of the oral cavity: εPKC, a novel prognostic factor for relapse and survival. Head Neck 1995;17:516–25.
9. Schechtman D, Mochly-Rosen D. Isozyme-specific inhibitors and activators of protein kinase C. Methods Enzymol 2002;345:470–89.
10. Mackay HJ, Twelves CJ. Protein kinase C: a target for anticancer drugs? Endocr Relat Cancer 2003;10:389–96.
11. Serova M, Ghoul A, Benhadji KA, et al. Preclinical and clinical development of novel agents that target the protein kinase C family. Semin Oncol 2006;33:466–78.
12. Nezhat F, Wadler S, Muggia F, et al. Phase II trial of the combination of bryostatin-1 and cisplatin in advance or recurrent squamous cell carcinoma of the cervix: a New York Gynecologic Oncology Group study. Gynecol Oncol 2004;93:144–8.
13. Peterson AC, Harlin H, Karrison T, et al. A randomized phase II trial of interleukin-2 in combination with four different doses of bryostatin-1 in patients with renal cell carcinoma. Invest New Drugs 2006;24:141–9.
14. Zhang J, Baines CP, Zong C, et al. Functional proteomic analysis of a three-tier PKC-ε-Akt-eNOS signaling module in cardiac protection. Am J Physiol Heart Circ Physiol 2004;288:H954–61.
15. Aziz MH, Manoharan HT, Verma AK. Protein kinase Cε, which sensitizes skin to sun's UV radiation-induced cutaneous damage and development of squamous cell carcinomas, associates with Stat3. Cancer Res 2007;63:1385–93.
16. Lim J, Kim JH, Paeng JY, et al. Prognostic value of activated Akt expression in oral squamous cell carcinoma. J Clin Pathol 2005;58:1199–205.
17. Massarelli E, Liu DD, Lee JJ, et al. Akt activation correlates with adverse outcome in tongue cancer. Cancer 2005;104:2430–6.
18. Shah NG, Trivedi TI, Tankshali RA, et al. Stat3 expression in oral squamous cell carcinoma: association with clinical parameters and survival. Int J Biol Markers 2006;21:175–83.
19. Hong FD, Clayman GL. Isolation of a peptide for targeted drug delivery into human head and neck solid tumors. Cancer Res 2000;60:6551–6.
20. Johnson JA, Gray MO, Chen C, Mochly-Rosen D. A protein kinase C translocation inhibitor as a isozyme-selective antagonist of cardiac function. J Biol Chem 1996;271:24962–6.
21. Csukai M, Chen CH, De Matteis MA, Mochly-Rosen D. The coatomer protein β'-COP, a selective binding protein (RACK) for protein kinase Cε. J Biol Chem 1997;272:29200–6.
22. Besson A, Wilson TL, Yong VW. The anchoring protein RACK1 links protein kinase Cε to integrin β chains. Requirements for adhesion and motility. J Biol Chem 2002;277:22073–84.
23. Yedovitzky M, Mochly-Rosen D, Johnson JA, et al. Translocation inhibitors define specificity of protein kinase C isoenzyme in pancreatic β-cells. J Biol Chem 1997;272:1417–20.
24. Hundle B, McMahon T, Dadgar J, Chen CH, Mochly-Rosen D, Messing RO. An inhibitory fragment derived from protein kinase Cε prevents enhancement of nerve growth factor responses by ethanol and phorbol esters. J Biol Chem 1997;272:15028–35.
25. Xiao GQ, Qu Y, Sun ZQ, Mochly-Rosen D, Boutjdir M. Evidence for functional role of εPKC isozyme in the regulation of cardiac Na(+) channels. Am J Physiol Cell Physiol 2001;281:C1477–86.
26. Brandman R, Disatnik MH, Churchill E, Mochly-Rosen D. Peptides derived from the C2 domain of protein kinase Cε (εPKC) modulate εPKC activity and identify potential protein-protein interaction surfaces. J Biol Chem 2007;282:4113–23.